

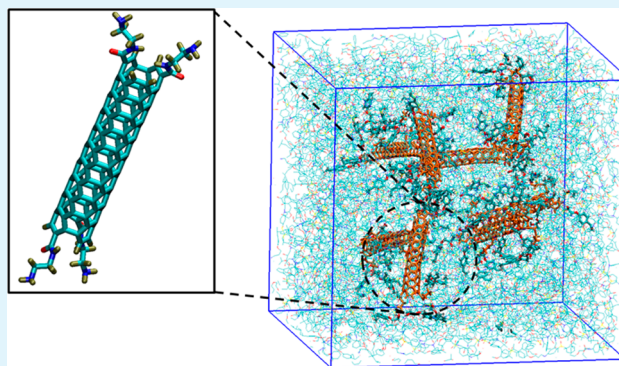
# Effect of Carbon Nanotube Functionalization on Mechanical and Thermal Properties of Cross-Linked Epoxy–Carbon Nanotube Nanocomposites: Role of Strengthening the Interfacial Interactions

Ketan S. Khare,<sup>†</sup> Fardin Khabaz, and Rajesh Khare\*

Department of Chemical Engineering, Texas Tech University, Lubbock, Texas 79409-3121, United States

**ABSTRACT:** We have used amido-amine functionalized carbon nanotubes (CNTs) that form covalent bonds with cross-linked epoxy matrices to elucidate the role of the matrix–filler interphase in the enhancement of mechanical and thermal properties in these nanocomposites. For the base case of nanocomposites of cross-linked epoxy and pristine single-walled CNTs, our previous work (Khare, K. S.; Khare, R. J. *Phys. Chem. B* **2013**, *117*, 7444–7454) has shown that weak matrix–filler interactions cause the interphase region in the nanocomposite to be more compressible. Furthermore, because of the weak matrix–filler interactions, the nanocomposite containing dispersed pristine CNTs has a glass transition temperature ( $T_g$ ) that is  $\sim 66$  K lower than the neat polymer. In this work, we demonstrate that in spite of the presence of stiff CNTs in the nanocomposite, the Young's modulus of the nanocomposite containing dispersed pristine CNTs is virtually unchanged compared to the neat cross-linked epoxy. This observation suggests that the compressibility of the matrix–filler interphase interferes with the ability of the CNTs to reinforce the matrix. Furthermore, when the compressibility of the interphase is reduced by the use of amido-amine functionalized CNTs, the mechanical reinforcement due to the filler is more effective, resulting in a  $\sim 50\%$  increase in the Young's modulus compared to the neat cross-linked epoxy. Correspondingly, the functionalization of the CNTs also led to a recovery in the  $T_g$  making it effectively the same as the neat polymer and also resulted in a  $\sim 12\%$  increase in the thermal conductivity of the nanocomposite containing functionalized CNTs compared to that containing pristine CNTs. These results demonstrate that the functionalization of the CNTs facilitates the transfer of both mechanical load and thermal energy across the matrix–filler interface.

**KEYWORDS:** functionalized carbon nanotubes, cross-linked epoxy nanocomposites, Young's modulus, matrix–filler interactions, thermal conductivity



## 1. INTRODUCTION

The remarkable mechanical properties<sup>1</sup> of carbon nanotubes (CNTs) have generated a large interest in the scientific community in the use of CNTs as fillers in polymer nanocomposites (PNCs), particularly in thermosetting polymers, such as cross-linked epoxy.<sup>2–4</sup> However, in general, the reinforcement of thermosetting matrices by CNTs has not lived up to the expectations.<sup>5</sup> On the theoretical side, the effect of CNTs on the physics of the polymer matrix is poorly understood.<sup>6</sup> This is partly because the wide variety of PNC preparation and processing strategies have significantly different effects on the properties of the final system, which has caused obstacles to comparing experimental results from various groups.<sup>7</sup> Furthermore, both cross-linked epoxy and CNTs are each a diverse class of materials, where the specific properties vary widely within these classes.

The glass transition temperature ( $T_g$ ) of the nanocomposites is an important signature of the effect of the filler on the thermo-viscoelasticity, and hence the physics of the polymer matrix.<sup>8</sup> The  $T_g$  is affected by the characteristics of the cross-

linked epoxy (specific chemistry, extent of conversion, etc.), the CNTs (number of walls, chemical functionalization, etc.), and the presence of additives (surfactants, processing agents, solvents, impurities, etc.). For example, the importance of the specific details of the cross-linked epoxy matrix topology can be seen in recent work, where it was found that the addition of multiwalled CNTs (MWNTs) to cross-linked epoxy results in either an increase or a decrease in the glass transition temperature ( $T_g$ ) in systems with low or high cross-link densities, respectively.<sup>9</sup> In a corresponding example regarding the importance of the specific details of CNT topology and chemical functionality, a recent review<sup>10</sup> noted that single walled CNTs (SWNTs) tended to cause a reduction in the

**Special Issue:** Applications of Hierarchical Polymer Materials from Nano to Macro

**Received:** November 23, 2013

**Accepted:** February 14, 2014

**Published:** March 7, 2014

glass transition temperature ( $T_g$ ) of the epoxy matrix, whereas MWNTs tended to cause an increase in the  $T_g$  of the matrix with respect to the neat polymer. However, the same review<sup>10</sup> included numerous exceptions to these generalizations, as well as a number of plausible hypotheses for the mechanisms that might cause changes in the  $T_g$  of the matrix because of the addition of the CNTs. Using experiments to verify these hypotheses by independently controlling these variables is challenging, because of the intricate interdependence of the associated phenomena, such as the extent of conversion, the extent of dispersion, and the effect of residual solvent and surfactants, etc.

Recently, we used molecular simulations to study systems in which the extent of dispersion of pristine SWNTs in a cross-linked epoxy nanocomposite system was independently varied.<sup>11</sup> This allowed us to study the volumetric, structural, and dynamic properties of the nanocomposites in the context of the specific interfacial interactions and the properties of the interphase region between the matrix and the filler, which is responsible for the load transfer between them. Briefly, we found that: (1) cross-linked epoxy and pristine CNTs have poor interfacial interactions, (2) the interphase between cross-linked epoxy and pristine CNTs is more compressible (as defined by the change in the specific volume with a change in the temperature) than the bulk matrix, (3) the creation of this interphase resulted in a large reduction in the  $T_g$  ( $\sim 66$  K) of the nanocomposite containing dispersed CNTs compared to the neat cross-linked epoxy, and (4) the effect of the filler on the dynamics of the matrix is nonintuitive. In addition, our observations provided support to the conceptual analogy between the nanoconfinement of the polymers by solid substrates and the effect of the filler on the matrix in the interphase region of PNCs that has been discussed in literature.<sup>12–17</sup>

In recent years, the significant progress in the chemistry of CNTs has enabled the attachment of a number of different functional groups and polymer chains to the surface of the CNTs.<sup>3</sup> In the case of cross-linked epoxy based CNT nanocomposites, the attachment of either epoxy<sup>18,19</sup> or amine<sup>20,21</sup> functional groups on the CNTs allows these CNTs to participate in the cross-linking reaction. In literature, the functionalization of CNTs with amine functional groups have been found to improve the mechanical properties of the cross-linked epoxy nanocomposites.<sup>21–25</sup> Such improvements in the mechanical properties due to the functionalization of CNTs has been mainly attributed to two factors: (1) improvement in the dispersion of the functionalized CNTs, and (2) improvement in the load transfer between the matrix and the filler because of the formation of covalent bonds and improved interfacial interactions between the matrix and the CNTs.<sup>1,22,26,27</sup> However, such functionalization of the CNTs in experiments is also known to reduce the extent of curing/conversion of the matrix,<sup>19,21</sup> shorten the length of the functionalized CNTs compared to the pristine CNTs,<sup>28,29</sup> and introduce significant amounts of impurities in the prepared material.<sup>20</sup> In addition, the oxidation-based functionalization of the CNTs is known to occur in a heterogeneous manner, with the edges of and defects in the CNTs being relatively rich in functional groups compared to the walls of the CNTs.<sup>3,30</sup> In this work, the use of molecular simulations has allowed us to use well-defined CNTs, and also to independently control the degree of conversion of the matrix, and the degree of dispersion of the CNTs without the use of additives such as surfactants

and dispersive agents. Therefore, we are able to separately decipher the effect of the covalent linkages between the cross-linked epoxy matrix and the functionalized CNTs on the mechanical properties of their nanocomposites. In addition, the use of atomistically detailed model structures for these systems allows us to fully account for the role of specific interfacial interactions between the matrix and the filler in these materials. Although specific chemical interactions are known to play an important role in the thermomechanical behavior of cross-linked epoxy systems;<sup>31</sup> the importance of accounting for these interactions is enhanced at the matrix–filler interface.<sup>6,32</sup>

The interfacial interactions between the matrix and the filler are also known to play a critical role in determining the ability of the filler to improve the thermal conductivity of the PNCs.<sup>33</sup> Specifically, CNTs are known to have an exceptionally high value of the thermal conductivity (single-walled CNTs,<sup>34</sup>  $\sim 6000$  W m<sup>-1</sup> K<sup>-1</sup>; and multiwalled CNTs,<sup>35,36</sup>  $\sim 3000$  W m<sup>-1</sup> K<sup>-1</sup>). On the other hand, polymers such as cross-linked epoxy have a low value of the thermal conductivity ( $\sim 0.3$  W m<sup>-1</sup> K<sup>-1</sup>).<sup>33</sup> Thus, while the use of the rule of mixtures would suggest a very large increase in the thermal conductivity of the matrix by the addition of a small amount of CNTs, the observed thermal conductivity of such nanocomposites reported in literature has been only marginally higher than the neat polymer.<sup>33</sup> This lack of significant improvement has been attributed to Kapitza resistance,<sup>37</sup> which is the thermal resistance between the matrix and the filler. Indeed, random walk Monte Carlo simulations have shown that the matrix–filler and filler–filler thermal resistances play a critical role in determining the overall thermal conductivity of the nanocomposite.<sup>36,38</sup> Functionalization of CNTs is expected to reduce the Kapitza resistance, by creating additional paths for the heat transfer between the matrix and the filler.<sup>39</sup>

We seek to answer the following two questions in this study: (1) What effect does the functionalization of CNTs have on the volumetric, structural, and dynamic properties in these nanocomposites?, and (2) How important is the nature of the interphase region in the overall load and heat transfer in these materials? To answer the first question, we created model structures of cross-linked epoxy nanocomposite containing dispersed functionalized CNTs, and then compared the volumetric, structural, and dynamic properties of this system with the corresponding properties of two model systems studied in previous work: neat cross-linked epoxy and the nanocomposite containing dispersed pristine CNTs.<sup>11,40</sup> To answer the second question, we calculated the mechanical properties of these model systems by simulating the deformation of the three systems described above, and also a fourth system: the nanocomposite containing aggregated pristine CNTs, which was previously characterized<sup>11</sup> for the volumetric, structural, and dynamic properties. In addition, the thermal conductivity of the four systems was also calculated using the reverse nonequilibrium molecular dynamics simulation (RNEMD) approach.<sup>41</sup>

This paper is organized as follows: we begin by describing the simulation details, which include a brief description of the preparation of the model structures of the nanocomposite containing amido-amine functionalized CNTs (FCNTs). This is followed by the results and discussion of the volumetric, structural, dynamic, mechanical, and thermal transport properties of the nanocomposite containing amido-amine functionalized CNTs, and a comparison of these properties with those of the neat cross-linked epoxy and the nanocomposites

containing pristine CNTs, which were prepared and studied in previous work.<sup>11,40</sup> We close the paper by summarizing the results in the Conclusions section.

## 2. SIMULATION DETAILS

The details of the force fields, molecular models, and the calculation of volumetric, structural, dynamic, mechanical, and thermal properties are presented in this section. In the simulations that are reported in this work, we use the acronym, “CNTs” to refer to pristine single-walled carbon nanotubes and the acronym, “FCNTs” to refer to amido-amine functionalized single-walled carbon nanotubes. The following abbreviations are used for the nanocomposite model systems in this paper: epoxy–disp. CNTs, epoxy–agg. CNTs, and epoxy–disp. FCNTs systems for the cross-linked epoxy nanocomposites containing dispersed pristine CNTs, aggregated pristine CNTs, and dispersed amido-amine functionalized CNTs, respectively.

**A. Force Fields and Molecular Models.** Similar to our previous studies,<sup>11,40</sup> the cross-linked epoxy network that constituted the polymer matrix was based on the epoxy monomer; diglycidyl ether of bisphenol A (DGEBA), and the cross-linker; 4,4'-diaminodiphenylsulfone (4,4'-DDS), as shown in panels a and b in Figure 1, respectively. Molecular models of the amido-amine functionalized CNTs (FCNTs) were prepared by adding two amido-amine groups<sup>29</sup> (i.e., –CONHCH<sub>2</sub>CH<sub>2</sub>NH<sub>2</sub>, see Figure 1c) to either end of the

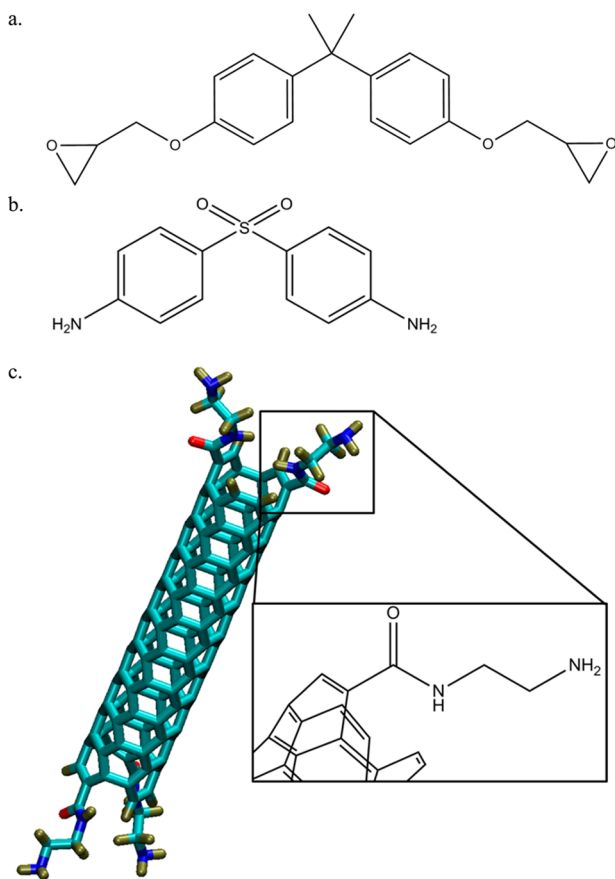


**Figure 1.** Chemical structures of (a) DGEBA and (b) 4,4'-DDS. (c) Molecular model of FCNTs used as the filler in this work. Carbon, oxygen, nitrogen, and hydrogen atoms are shown in cyan, red, blue, and gray color, respectively. Inset contains the chemical structure of the amido-amine functional group.

pristine single-walled CNTs of chirality (3,3). These pristine CNTs were used in our previous simulation work,<sup>11</sup> and the amido-amine functional groups have been used in literature experiments.<sup>28,42</sup> We note that because each of the amido-amine groups can form three covalent bonds with the matrix, rather than the one covalent bond that would be formed if the functional group was epoxy, the former is expected to be more effective for improving the matrix–filler load and heat transfer.

As can be seen in Figure 1c, four amido-amine groups were attached to each FCNT. Thus, the number of CNT carbon atoms per functional group was 30, which is similar to the number of CNT carbon atoms per functional group used in experimental work in literature.<sup>20</sup> Each of these amido-amine groups can react with three epoxy functional groups from the matrix during the cross-linking process. This aspect was taken into account while calculating the stoichiometric ratio of the epoxy and the amine groups in the reaction mixture during the preparation of the cross-linked model structures, the details of which are given in the subsequent text. These stoichiometric considerations are important for avoiding a reduction in the extent of curing because of the presence of the unreacted excess component, which has been thought to be one of the possible reasons for a reduction in the  $T_g$  of the nanocomposite that has been observed in experimental literature.<sup>21</sup>

Although the simulation details of the work presented here are similar to those for our previous studies,<sup>11,40</sup> we briefly summarize some key features for the sake of completion. The intra- and intermolecular forces that govern the behavior of the molecular models were described by the general AMBER force field<sup>43,44</sup> (gAff). The partial charges on the atoms were determined using the AM1-BCC method.<sup>45,46</sup> We have previously used these methods to simulate various cross-linked epoxy systems and their nanocomposites, and have shown that the simulated properties are in excellent agreement with experimental literature.<sup>11,40,47–50</sup> The van der Waals and Columbic interactions were considered explicitly up to a cutoff distance of 9 Å. Beyond this cutoff distance, we used tail corrections and the particle–particle particle–mesh<sup>51</sup> (PPPM) algorithm to account for the respective long-range interactions. All the constant pressure simulations were performed at a pressure of 1 atm. The Nosé–Hoover thermostat and barostat were used to control the temperature and pressure, respectively.<sup>52</sup> All of the simulations reported in this work were performed using the LAMMPS simulation package.<sup>53</sup> A time-step of 1 fs was used for the MD simulations.<sup>54</sup>

**B. Preparation of Model Structures.** Model structures of the epoxy–disp. FCNTs system were prepared in this work (see Figure 2) and properties of these systems were compared with properties of the model systems of the neat cross-linked epoxy, the epoxy–disp. CNTs, and the epoxy–agg. CNTs systems that were described in our previous work.<sup>11,40</sup> To maintain stoichiometry of the epoxy and amine groups, we used 896 molecules of DGEBA, 424 molecules of DDS, and 8 FCNTs to prepare the “reaction mixture”; the mass fraction of FCNTs thus is 3.4 and 2.75%, calculated with and without the functional group atoms, respectively. This initial reaction mixture was simulated at 553 K using constant  $NPT$  (constant number of particles, pressure, and temperature) simulations. The directed diffusion-based simulated polymerization<sup>40</sup> approach was then used to prepare the nanocomposite containing FCNTs. The extent of dispersion of the filler in the epoxy–disp. FCNTs system was identical to that in the epoxy–disp. CNTs system.<sup>11</sup> The procedure for dispersing the

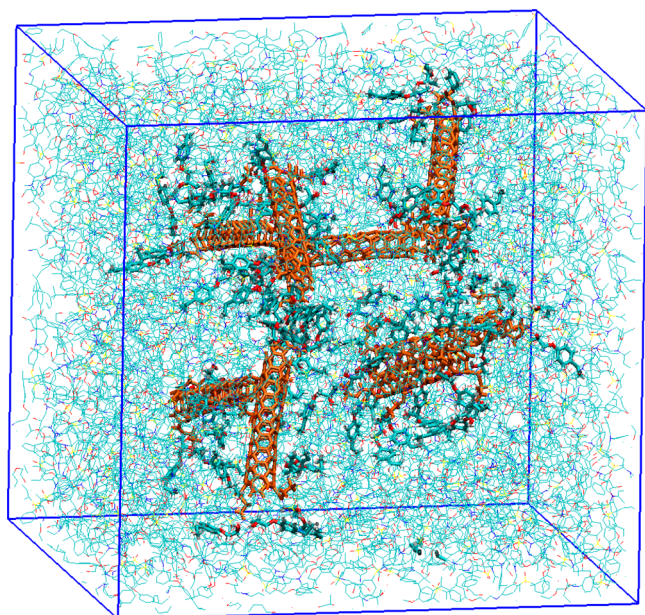


**Figure 2.** Snapshot of the epoxy-disp. FCNTs nanocomposite structure. The FCNTs are shown in orange color. Carbon, hydrogen, oxygen, nitrogen, and sulfur atoms are shown in cyan, white, red, blue, and yellow color, respectively. The DGEBA units with covalent attachments to the FCNTs are represented by thicker bonds, whereas hydrogen atoms are not shown for clarity.

FCNTs, as well as the simulated polymerization was identical to the preparation<sup>11</sup> of the epoxy-disp. CNTs system, with a few modifications that were required to account for the creation of covalent bonds between these FCNTs and the matrix. Specifically, the four amido-amine groups on each of the FCNTs were expected to react with twelve units of the epoxy monomer DGEBA. These covalent bonds were created before the simulated polymerization of the rest of the “reaction mixture”, i.e., the formation of bonds between DGEBA and 4,4'-DDS using the directed diffusion based simulated polymerization.<sup>40</sup> The extent of conversion of the matrix for the model structures of the epoxy-disp. FCNTs system is compared with those of the previously studied systems<sup>11,40</sup> in Table 1.

**Table 1.** Comparison of the Extent of Chemical Conversion of the Epoxy-Disp. FCNTs System with the Conversion of the Systems Studied in Previous Work

system	extent of conversion
neat cross-linked epoxy <sup>40</sup>	0.989 ± 0.0036
epoxy-disp. CNTs <sup>11</sup>	0.987 ± 0.0055
epoxy-agg. CNTs <sup>11</sup>	0.994 ± 0.0018
epoxy-disp. FCNTs	0.988 ± 0.0015

### C. Volumetric, Structural, and Dynamic Properties.

The volumetric, structural, and dynamic properties of the cross-linked epoxy and the epoxy-disp. CNTs system, which were obtained in the previous studies,<sup>11,40</sup> are compared with the corresponding properties of the epoxy-disp. FCNTs system that are calculated in this work. The epoxy-disp. CNTs and the epoxy-disp. FCNTs systems have similar morphology other than the presence of the covalent bonds between the CNTs and the matrix in the latter but their absence in the former. Therefore, by focusing primarily on the comparison between

these two systems, we were able to independently decipher the effect of the functionalization of the CNTs on the thermomechanical properties of the nanocomposites.

Although the details of these calculations are similar to our previous work,<sup>11,40</sup> for the sake of completion, we summarize the key features of these calculations for the three properties. The specific volume of the epoxy-disp. FCNTs system was obtained by a stepwise cooling process (step-size: 20 K) of the model structures starting from a high temperature in the rubbery state ( $T = 763$  K). A constant  $NPT$  simulation was performed for 2 ns in each step, and the volumetric data was collected in the last half of each of these cooling steps. At the end of each temperature step, a snapshot of the model structures was saved for further calculations.

The radial distribution function of the heavy atoms in the matrix in cylindrical shells around the FCNTs was calculated and compared with a similar quantity in previous work<sup>11</sup> for the epoxy-disp. CNTs system. For the dynamic properties, the mean-squared displacement (MSD) was calculated for the central carbon atoms of DGEBA units and the nitrogen atoms of the DDS units, which are expected to be the fastest and the slowest atoms in the matrix, respectively. The MSD was also calculated for the carbon atoms of the FCNTs. These calculations were performed at a temperature of 454 and 494 K, the same as those in the previous work on neat cross-linked epoxy, epoxy-disp. CNTs, and epoxy-agg. CNTs systems.<sup>11</sup>

**D. Determination of Mechanical Properties.** The mechanical properties were characterized by calculating the Young's modulus ( $E$ ) and the Poisson ratio of the four model systems: (1) neat cross-linked epoxy, (2) epoxy-disp. CNTs, (3) epoxy-agg. CNTs, and (4) epoxy-disp. FCNTs systems, by simulating the uniaxial deformation of these systems. For this purpose, we used the well-relaxed model structures obtained during the stepwise cooling simulations that were carried out for studying the volume – temperature behavior. Five replicas of each of the four systems were deformed in each of the three Cartesian directions in both a compressive and tensile manner, thus allowing us to obtain the Young's modulus and Poisson ratio as an average of 30 simulations for each of the four systems.

The uniaxial deformation was simulated at a constant engineering strain rate of  $1 \times 10^6$  s<sup>-1</sup> and at a temperature of 300 K, i.e., deep in the glassy state. Concurrently with this deformation, a constant  $NPT$  simulation was performed to allow the model systems to relax. The Nosé-Hoover barostat<sup>52</sup> was applied to the dimensions lateral to the deformation with a target pressure of 1 atm. Such a process allows the lateral dimensions to adjust to the longitudinal deformation based on the relaxation of the model structures, enabling us to calculate the Poisson ratio. Two of us recently used this method to characterize the mechanical response of a different cross-linked epoxy system as a function of the strain rate and the temperature.<sup>50</sup>

**E. Calculation of Thermal Conductivity.** The thermal conductivity of the four model systems was calculated using the reverse nonequilibrium molecular dynamics<sup>41</sup> (RNEMD) method, which has been implemented in the LAMMPS simulation package.<sup>53</sup> The RNEMD method<sup>41</sup> relies on generating a thermal gradient in response to an imposed steady heat flux. This steady heat flux is induced by swapping the velocities of the hottest (particle with the highest velocity) and the coldest (particle with the lowest velocity) particles, which belong to predefined cold and hot slab regions of the

simulation box. This swapping process is repeated at a specified time interval, which on average creates a constant heat flux, and consequently results in the establishment of a thermal gradient. This time interval is chosen such that the temperature difference across the simulation box is relatively small. Specifically, in our work, we used a time interval of 120 time steps, which allowed us to maintain a temperature difference of less than 30 K across the simulation box. Maintaining a small temperature difference allowed us to neglect the temperature dependence of the thermal conductivity and thus assume that the thermal conductivity was a constant for the model structure at the average temperature of the simulation. The thermal conductivity of the system was then calculated by dividing the measured heat flux by the average temperature gradient. The average thermal conductivity was obtained by performing these calculations along each of the three directions for each of the five replicas of the four model systems. For the thermal conductivity calculations, the well-relaxed structures obtained at a temperature of 303 K and pressure of 1 atm were subjected to constant *NVE* simulations for a duration of 4 ns.

### 3. RESULTS AND DISCUSSION

We begin by reporting the volumetric, structural, and dynamic properties of the epoxy–disp. FCNTs system. These results are compared with previous work on neat cross-linked epoxy<sup>40</sup> and the epoxy–disp. CNTs systems.<sup>11</sup> These discussions are followed by a comparison of the Young's modulus, the Poisson ratio, and the thermal conductivity of these three model systems along with the epoxy–agg. CNTs system. In all cases, the uncertainty in the results was determined by averaging over 5 replicas for each of the four model systems.

**A. Functionalization of CNTs Eliminates the  $T_g$  Depression Shown by Dispersed Pristine CNTs in Their Cross-linked Epoxy Nanocomposites.** The model structures of the epoxy–disp. FCNTs system were relaxed at a high temperature ( $T = 783$  K) using a constant *NPT* molecular simulation and then subjected to a stepwise cooling procedure. The cooling rate used in these simulations is  $1 \times 10^{10}$  K s<sup>-1</sup>, which is identical to that in our previous work.<sup>11,40</sup> In Figure 3, the dependence of the specific volume of the epoxy–disp. FCNTs system with the temperature is compared on our previous results for neat cross-linked epoxy<sup>40</sup> and the epoxy–disp. CNTs systems.<sup>11</sup> As can be seen from the figure, the epoxy–disp. FCNTs system has significantly lower specific volume (i.e., significantly higher density) than the other two systems. The  $T_g$  was estimated by determining the temperature at the intersection of the linear fits to the rubbery (603–763 K) and the glassy regions (303–403 K). As can be seen, the value of  $T_g$  of the epoxy–disp. FCNTs system ( $T_g = 517 \pm 23$  K) is significantly higher than the  $T_g$  of the epoxy–disp. CNTs system ( $T_g = 446 \pm 12$  K). On the other hand, the  $T_g$  of the epoxy–disp. FCNTs system is comparable to that of the neat cross-linked epoxy ( $T_g = 512 \pm 13$  K), within the uncertainties associated with those values. Since the extent of dispersion of the filler in the case of the epoxy–disp. CNTs and the epoxy–disp. FCNTs systems is identical, this suggests that the functionalization of the CNTs eliminates the  $T_g$  depression shown by the epoxy–disp. CNTs system compared to the neat cross-linked epoxy. This  $T_g$  depression was attributed to poor interfacial interactions between the pristine CNTs and the cross-linked epoxy in our previous work.

**B. Functionalization of CNTs Renders the Interphase More Incompressible.** A comparison of the temperature

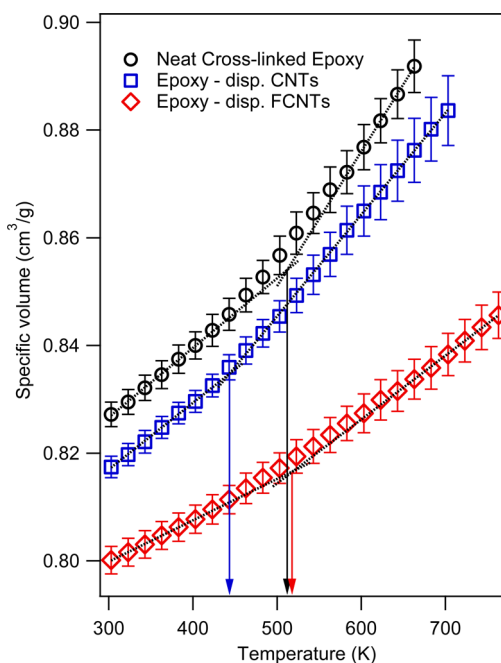


**Figure 3.** Comparison of the volume–temperature data of cross-linked epoxy–disp. FCNTs system with data obtained in previous studies for the neat cross-linked epoxy<sup>40</sup> and the epoxy–disp. CNTs system.<sup>11</sup>

dependence of the specific volume of the epoxy–disp. CNTs and the epoxy–disp. FCNTs systems can be used to obtain more information about the effect of the functionalization on the compressibility of the interphase region. In previous work,<sup>11</sup> we have defined the quantity: excess specific volume ( $V_{\text{excess}}$ ) to quantify the difference between the specific volume of the epoxy–disp. CNTs and epoxy–agg. CNTs systems at a given temperature. In that work, since the other characteristics of the two systems, such as the mass fraction of the CNTs, were the same, this excess specific volume arose exclusively because of a difference in the extent of dispersion of the CNTs in the two systems. Thus, in that work,<sup>11</sup> the value of the  $V_{\text{excess}}$  as well as its dependence on the temperature led us to conclude that the interphase region between pristine CNTs and the cross-linked epoxy matrix is compressible. This conclusion was possible because the only difference between those two model systems was the volume fraction of the interphase, which was caused by the aforementioned differences in the extent of dispersion.

In this work, the value of the  $V_{\text{excess}}$  between the epoxy–disp. CNTs and epoxy–disp. FCNTs systems which can be calculated at a given temperature, will have a subtly different interpretation than that in our previous work.<sup>11</sup> Here, since the difference between the two models (i.e., epoxy–disp. CNTs and epoxy–disp. FCNTs systems) is in the nature of the interphase and not the volume fraction of the interphase region, this quantity can be used to assess the effect of the change in the nature of the interphase on the relative compressibility of the two interphase regions. In particular, here we define the excess specific volume as:  $V_{\text{excess}} = 2(V_{\text{disp}} - V_{\text{funct}})/(V_{\text{disp}} + V_{\text{funct}})$ . The trend in  $V_{\text{excess}}$  with a change in temperature is shown in Figure 4. It can be seen from Figure 4 that the use of pristine CNTs compared to the functionalized CNTs results in an excess specific volume due to the nature of the interphase for these systems. Furthermore, the  $V_{\text{excess}}$  monotonically decreases with a decrease in temperature for these systems. This trend suggests that the interphase formed by the cross-linked epoxy

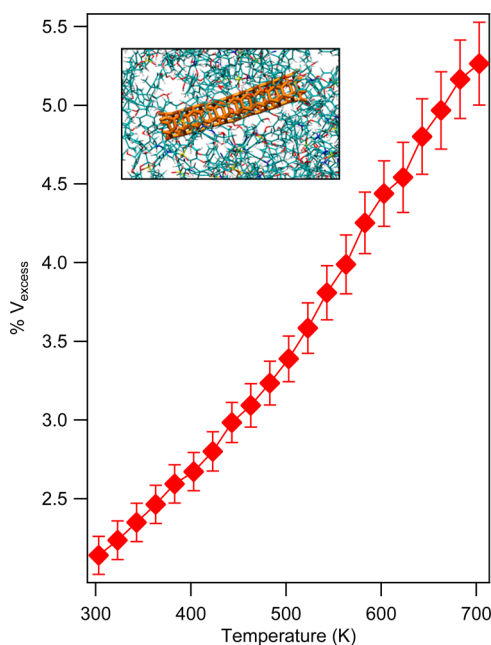


**Figure 4.** Temperature dependence of the excess specific volume of the epoxy-disp. CNTs system with respect to epoxy-disp. FCNTs system.

matrix and the amido-amine functionalized CNTs has significantly lower compressibility than the interphase formed by cross-linked epoxy matrix and the pristine CNTs. (Note: Compressibility is defined here in terms of the change in the volume with respect to a change in the temperature.) This observation is consistent with the expectation that functionalization of CNTs increases the compatibility between the matrix and the filler. Indeed, amido-amine functionalized CNTs have been reported in the literature to be more compatible with the cross-linked epoxy compared to pristine CNTs.<sup>22,27</sup>

**C. Local Structure of Matrix is Unaffected by Functionalization of CNTs.** In previous work, we found that poor compatibility of the matrix and the filler in the epoxy-disp. CNTs system did not result in the depletion of the matrix atoms around the filler. In order to determine the effect of FCNTs on the local matrix structure, the radial distribution function (RDF) of the heavy atoms of the matrix in cylindrical shells around the FCNTs was calculated at a temperature  $T = 494$  K. Figure 5 presents a comparison of this RDF with a similar RDF<sup>11</sup> for the heavy atoms of the matrix in cylindrical shells around the pristine CNTs in the epoxy-disp. CNTs system. As can be seen from the figure, the functionalization of the CNTs did not result in large changes in the local structure of the matrix of the epoxy-disp. FCNTs system as compared to that in the epoxy-disp. CNTs system. Specifically, neither the height of the first peak, nor the location of the first peak showed significant changes. The functionalization of the CNTs did allow a few more matrix atoms to reside spatially close to the CNTs as can be seen by comparing the values of the RDF at distances less than  $\sim 5$  Å. However, it is clear that the RDF is poorly correlated with interfacial interactions, as was also reported by us in previous work,<sup>11</sup> and as is indicated by the literature on water containing systems in the field of biophysics.<sup>55</sup> Although the local structure of the matrix around the filler is relatively unaffected by the functionalization of the filler, the dynamic properties are expected to be more

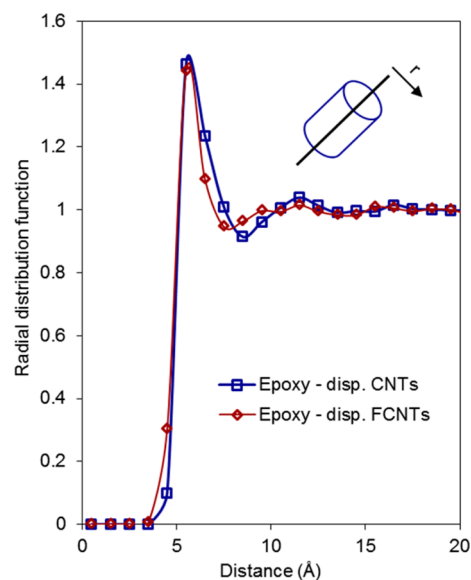


**Figure 5.** Comparison of the RDF of heavy atoms of the polymer matrix around the carbon atoms of the CNTs for the epoxy-disp. FCNTs system at a temperature of 494 K with a similar RDF for epoxy-disp. CNTs system reported in previous work.<sup>11</sup> The error bars (not shown) are of the size of the symbols.

significantly affected by the presence of the covalent bonds between the matrix and the filler.

**D. Functionalization of the Filler Suppresses the Mobility of Matrix Atoms.** The effect of the CNTs on the dynamics of atoms in the polymer matrix is nonintuitive, as reported in our previous work,<sup>11</sup> and as reviewed elsewhere.<sup>6</sup> Because we had previously assessed the effect of pristine single-walled CNTs on the mobility of the matrix atoms in cross-linked epoxy nanocomposites, a similar assessment in the epoxy-disp. FCNTs system will allow us to decipher the effect of functionalization of CNTs on this aspect. Similar to our previous work,<sup>11</sup> we calculated the MSD of the central carbon atoms of DGEBA units at a temperature of 494 K in the epoxy-disp. FCNTs system and compared it with the corresponding value for the epoxy-disp. CNTs system from our previous work,<sup>11</sup> as shown in Figure 6. The central carbon atoms of DGEBA units were chosen for analysis because these are expected to be the most mobile atoms in the matrix.<sup>47</sup> As can be seen in Figure 6, functionalization of the CNTs had a strong effect of reducing the translational mobility of the matrix atoms. Specifically, the MSD of the matrix atoms in the epoxy-disp. FCNTs system is a factor of 3 lower than that of both the neat cross-linked epoxy and the epoxy-disp. CNTs system. This reduction can be attributed to (1) the higher density of the epoxy-disp. FCNTs system compared to both the neat cross-linked epoxy and the epoxy-disp. CNTs systems, and (2) the presence of multiple functional groups on the filler, the resulting covalent bonds are likely to cause a significant reduction in the mobility within the matrix.

**E. Covalent Bonds between Functional Groups and Matrix Pin the FCNTs in the Matrix.** The MSD of the carbon atoms of the FCNTs will provide additional insight into effect of the covalent bonds between the matrix and the filler on the dynamics of the filler. Figure 7 shows the temporal evolution of the value of the MSD of the carbon atoms of the FCNTs in the epoxy-disp. FCNTs system; the figure also shows a comparison of these data with a similar trend for the

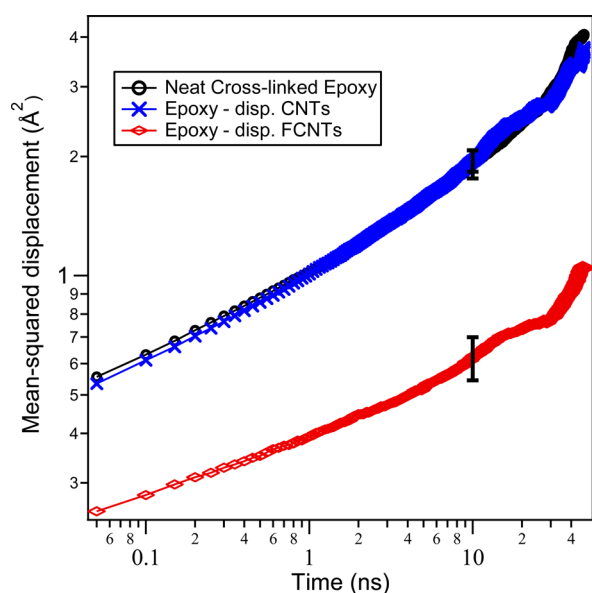


**Figure 6.** Comparison of the MSD of central carbon atoms on DGEBA units in the epoxy–disp. FCNTs system at a temperature of 494 K with the corresponding MSDs in the neat cross-linked epoxy and the epoxy–disp. CNTs systems from previous work.<sup>11</sup>

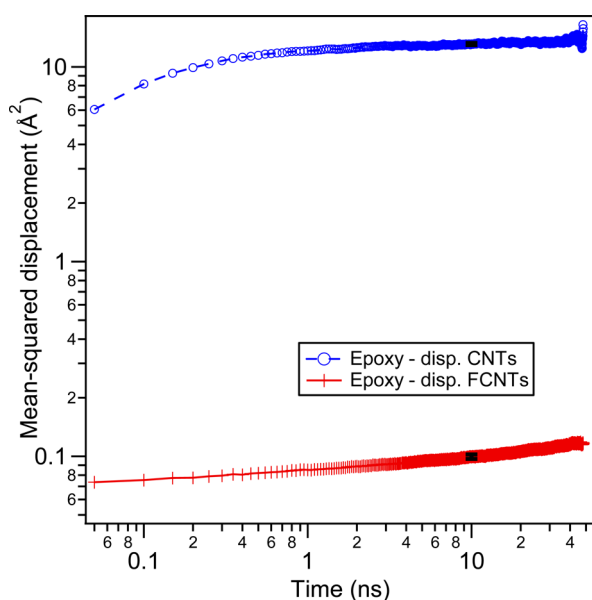


**Figure 7.** Comparison of the MSD of carbon atoms on CNTs in the epoxy–disp. FCNTs system at a temperature of 494 K with the corresponding MSD in the epoxy–disp. CNTs system from previous work.<sup>11</sup>

CNT atoms in the epoxy–disp. CNTs system studied in our previous work.<sup>11</sup> As can be seen from Figures 6 and 7, the presence of covalent bonds between the matrix and the FCNTs fundamentally changes the nature of the dynamics between the two phases. The drastic reduction in the MSD of atoms of FCNTs compared to pristine CNTs, which can be seen in Figure 7, suggests that the covalent bonds between the functional groups of the FCNTs and the matrix had an effect of pinning the FCNTs to the matrix. The 12 connections between each of the FCNTs and the matrix effectively render the FCNTs immobile. On the other hand, the mobility of the carbon atoms on the pristine CNTs is significantly higher than

the matrix atoms on shorter time-scales, which is indicative of a decoupling of dynamics between the filler and the matrix in that system. Our observations are consistent with an experimental study<sup>24</sup> of the variations in the Raman spectra of both the pristine and the amine functionalized MWNTs in their cross-linked epoxy nanocomposites, respectively, as a function of the tensile strain. Specifically, it was found that under the tensile deformation, the interatomic distances of the carbon atoms in the pristine MWNTs were unaffected, indicating that the dynamics of the matrix and the filler were uncorrelated. On the other hand, these distances were affected by the application of the tensile deformation in the case of the nanocomposite containing amine functionalized MWNTs, suggesting that the matrix–filler dynamics were coupled.

**F. Compressible Interphase Between the Matrix and Pristine CNTs Interferes in the Mechanical Load Transfer.** The coupling of the dynamics of the matrix and the filler in the case of the epoxy–disp. FCNTs system can be expected to facilitate load transfer between the epoxy matrix and the FCNTs. As described in the previous section, the mechanical properties of these four systems were calculated by applying uniaxial deformation at a strain rate of  $1 \times 10^6 \text{ s}^{-1}$  on the well-relaxed structures of each system at a temperature of 300 K, which is deep in the glassy state for all of these systems. In particular, we calculated the Young's modulus and the Poisson ratio for these systems, which are shown in Table 3.

**Table 3.** Glass-Transition Temperature ( $T_g$ ), Young's Modulus ( $E$ ), Poisson Ratio ( $\nu$ ), and the Bulk Modulus ( $B$ ) of Neat Cross-Linked Epoxy and the Three Nanocomposite Systems<sup>a</sup>

system	$T_g$ (K)	$E$ (GPa)	$\nu$	$B$ (GPa)
cross-linked epoxy	$512 \pm 13$	$5.74 \pm 0.14$	$0.368 \pm 0.003$	$7.25 \pm 0.19$
epoxy–disp. CNTs	$446 \pm 12$	$5.70 \pm 0.32$	$0.379 \pm 0.003$	$7.85 \pm 0.45$
epoxy–agg. CNTs	$499 \pm 5$	$6.47 \pm 0.45$	$0.363 \pm 0.004$	$7.87 \pm 0.55$
epoxy–disp. FCNTs	$517 \pm 23$	$8.63 \pm 0.21$	$0.343 \pm 0.007$	$9.16 \pm 0.29$

<sup>a</sup>The mechanical properties reported here were obtained at a temperature of 300 K.

As can be seen in that table, the value of  $E$  for the neat cross-linked epoxy is calculated to be  $5.74 \pm 0.14$  GPa. In recent work,<sup>50</sup> two of us have shown that the value of the  $E$  in the glassy state calculated using simulations is expected to be  $\sim 2$  GPa higher than that obtained in experiments. This difference in the value of  $E$  arises from the overlap of the  $\alpha$  and the  $\beta$  relaxation modes at the high strain rates that are used in simulations and their separation at lower strain rates that are employed in experiments. In particular, at the typical deformation conditions used in experiments ( $\sim 1$  Hz), the  $\beta$  peak temperature for the cross-linked epoxy system used in our work is reported to be 229 K.<sup>31</sup> This  $\beta$  peak temperature shifts to higher values with higher strain rates, thus at the strain rate of  $1 \times 10^6 \text{ s}^{-1}$  that is used in these simulations, the  $\beta$  peak temperature is expected to be greater than 300 K, i.e.,  $\beta$  relaxation does not occur at the simulation conditions.<sup>50</sup> Because the value of the Young's modulus increases by about 2 GPa as temperature is lowered from a value higher than the  $\beta$

relaxation peak temperature to a lower value,<sup>56</sup> the simulated value of  $E$  reported here is in good agreement with experimental value ( $E = 2.79 \pm 0.03$  GPa) reported in literature for the same cross-linked epoxy system.<sup>31</sup>

In the case of the epoxy–disp. CNTs system, despite the excellent dispersion of the stiff CNTs, the value of  $E$  for that system is comparable to that of the neat cross-linked epoxy. This observation suggests that the reinforcement of the matrix due to the stiff filler is negated by the compressible interphase region between them. On the other hand, the epoxy–agg. CNTs system showed a value of  $E$  that was  $\sim 12\%$  higher than that of both the neat cross-linked epoxy and the epoxy–disp. CNTs system. We attribute this observation to the presence of a smaller amount of the compressible interphase in this system due to the aggregation of the CNTs. The lower values of both the  $T_g$  and the  $E$  of the epoxy–disp. CNTs system, as well as the higher value of its Poisson ratio compared to the corresponding properties of the epoxy–agg. CNTs system suggests that the former is more ductile<sup>57</sup> than the latter at a given temperature below their  $T_g$ . This inference agrees with experimental literature,<sup>58</sup> where it was reported that the nanocomposite containing well-dispersed MWNTs was more “liquid-like” than the nanocomposite containing aggregated MWNTs. With regard to this comparison, we note that the term “dispersion”, in experiments, usually refers to “macro-dispersion”, i.e., the dispersion of clusters of CNTs throughout the experimental sample, unlike the dispersion of individual CNTs (i.e., “nanodispersion”),<sup>59</sup> which is the case in the present simulation work. In literature,<sup>60</sup> simulations of a coarse-grained linear polymer and its nanocomposite were observed to show significantly lower values of  $E$  under a tensile deformation than those calculated under a compressive deformation. In our work, given the uncertainty associated with the calculation, no systematic trend is observed between the values of  $E$  calculated under tensile and compressive deformations. We attribute this lack of a significant difference between the two values of  $E$  observed by us to the highly cross-linked nature of the matrix used in this work, unlike the study reported in literature, where a system of linear chains was used.<sup>60</sup>

**G. Functionalization of CNTs Facilitates the Load Transfer Between the Matrix and the Filler.** As previously discussed, the epoxy–disp. FCNTs system shows a value of the  $T_g$  that is similar to that of the neat cross-linked epoxy, and the interphase region in that system was relatively incompressible as compared to that in the epoxy–disp. CNTs system. As can be seen in Table 3, the functionalization of the CNTs resulted in  $\sim 50\%$  increase in the value of  $E$  of the system compared to both the neat cross-linked epoxy and the epoxy–disp. CNTs system. This observation indicates that the incompressible interphase between the FCNTs and the matrix was more effective at load transfer than the compressible interphase between the pristine CNTs and the matrix. Indeed, our observations agree with several papers in literature that have reported that amine functionalized CNTs are effective at reinforcing cross-linked epoxy matrices, whereas pristine CNTs are not.<sup>21–25</sup>

The Halpin–Tsai<sup>61</sup> model has been used in literature<sup>25</sup> to estimate the value of  $E$  of cross-linked epoxy–CNT nanocomposites. If the filler is assumed to be randomly oriented in the three directions, and the value of  $E$  for the neat cross-linked epoxy and the CNTs are taken to be 5.74 GPa and 1 TPa from the present work and literature,<sup>1</sup> respectively, the  $E$  for the nanocomposite can be estimated to be 6.71 GPa using the

Halpin–Tsai model. In the case of the epoxy–disp. CNTs system, the simulated value of  $E$  is lower than the Halpin–Tsai model estimates, while in the case of the epoxy–disp. FCNTs system, the simulated value of  $E$  is significantly higher than the model estimate. The inability of the Halpin–Tsai model to predict these differences between the value of the  $E$  of the epoxy–disp. CNTs and the epoxy–disp. FCNTs systems can be attributed to the neglect of the matrix–filler interfacial interactions and the associated interphase in the Halpin–Tsai model. Thus, the Halpin–Tsai model is unable to account for the changes in the thermoviscoelastic properties of the nanocomposites that are likely to occur because of the creation of an interphase.<sup>8</sup>

For isotropic and viscoelastic materials,<sup>62</sup> the value of the Bulk modulus ( $B$ ) can be calculated from the Young’s modulus ( $E$ ) and the Poisson ratio ( $\nu$ ) by the following relationship:  $B = E/3(1 - 2\nu)$ . The value of  $B$  is of particular interest to our discussion of the compressibility of the interphase, because  $B$  is simply the inverse of the compressibility, albeit for the entire system consisting of the CNT, interphase region and the bulk epoxy matrix. In Table 3, the values of the  $B$  for the four systems so calculated from  $E$  and  $\nu$  values are presented. As can be seen, the epoxy–disp. FCNTs system has a value of  $B$  which is  $\sim 17\%$  higher than that of the epoxy–disp. CNTs system. Because the only difference between the two systems is the nature of the matrix–filler interphase, this higher value of  $B$  can be directly attributed to the higher incompressibility of the matrix–filler interphase in the case of the epoxy–disp. FCNTs system compared to the epoxy–disp. CNTs system. The relatively high uncertainty associated with the calculation of  $B$  and mechanical properties in general, makes it difficult to draw any conclusion about the relative trend in  $B$  values for the epoxy–disp. CNTs and the epoxy–agg. CNTs systems. The  $B$  value of the epoxy–disp. CNTs system appears to be slightly higher than that of the neat cross-linked epoxy system but such a comparison is complicated by the opposing effects of two factors: presence of both the compressible interphase as well as the stiff CNT fillers in the former system, and the absence of these two in the latter.

In summary, we note that  $B$  values can be used to derive conclusions about the compressibility of the interphase region in the nanocomposite systems. In practice, such an application of  $B$  values is complicated by factors such as the high uncertainty in calculation of the mechanical properties in simulations and the presence of stiff nanofillers in the system. In comparison, the calculation of the volumetric properties is associated with significantly less uncertainty in simulations than the calculation of the mechanical properties. We thus assert that the trend in the excess free volume with temperature discussed in the previous<sup>11</sup> and the present work is a more sensitive measure of the compressibility of the interphase region than the Bulk modulus.

**H. Heterogeneities in the Nature of the Interphase Could Explain the Occurrence of Craze in Epoxy-Based Nanocomposites.** Our results can also provide molecular insight into a recent report<sup>28</sup> of the occurrence of crazing in cross-linked epoxy reinforced by amido-amine functionalized CNTs. In the use of polymeric materials for structural applications, the occurrence of crazing during deformation leads to significant energy dissipation.<sup>63</sup> As a result, the fracture toughness of these materials is significantly enhanced and material failure is delayed, which are desirable characteristics for structural applications. Craze is a “micro-



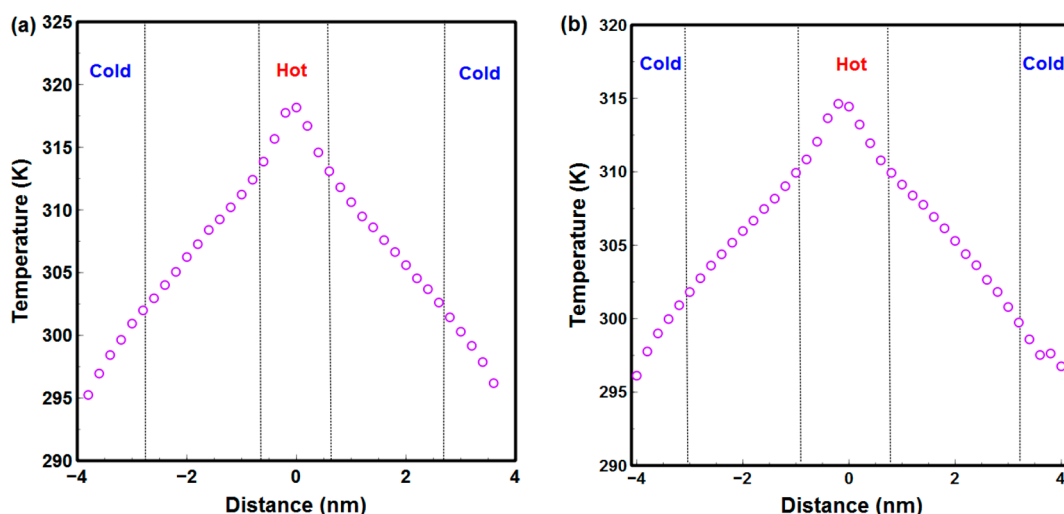


**Figure 8.** Temperature profiles for (a) cross-linked epoxy and (b) epoxy–disp. FCNTs systems.

scopically localized” phenomenon that involves a highly concentrated state of localized stresses and is driven by the formation of drawn fibrils of the polymer that span the interfaces of load bearing cracks in the polymer.<sup>63</sup> The presence of defects and contaminants often amplifies this localized stress concentration and hence, promotes the occurrence of crazing.<sup>63</sup> Local heterogeneities in the polymer, whether intrinsic to the polymer or extrinsic (induced by the addition of fillers) are considered to be essential for the observation of crazing.<sup>63</sup> In the case of filler reinforced polymers, filler-induced changes in the local  $T_g$  (and correspondingly, local free volume and local dynamics) of the matrix have been suggested to drive the formation of fibrils.<sup>64</sup> Indeed, crazing was also recently studied using coarse-grained molecular simulations of linear polymer chains with rodlike fillers, where the filler was found to lead to premature crazing compared to the neat polymer.<sup>65</sup>

Because cross-linked epoxy is a thermoset, it is a rather stiff, but not a particularly tough material, and crazing is typically not observed in this material.<sup>66–68</sup> However, in recent experimental work, crazing in cross-linked epoxy reinforced by amido-amine functionalized MWNTs (A-MWNTs) was observed.<sup>28</sup> In that same work, crazing was not observed in both the neat cross-linked epoxy and cross-linked epoxy reinforced by pristine MWNTs. Furthermore, it was reported that the fibrils observed during crazing in the nanocomposite containing A-MWNTs were primarily comprised of the matrix material, and not the A-MWNTs. This observation suggests that the A-MWNTs did not directly participate in the crazing process; rather the A-MWNTs modified the thermomechanical response of the matrix to the deformation by inducing local heterogeneities in the cross-linked epoxy matrix.

In the case of experimental samples of A-MWNTs, amido-amine functionalization tends to occur near the edges of CNTs.<sup>3,21,29</sup> Thus, it is reasonable to expect that there are significant local heterogeneities in the thermo-mechanical character of the interphase between the matrix and the filler in experimental samples of the nanocomposites. Within the same experimental sample of the nanocomposite containing A-MWNTs, different locales in the material can be expected to exhibit the thermo-mechanical characteristics resembling those of the four model systems that were studied in this work. Specifically, across the four systems, large variations were found in the density (1.209–1.250 g/cm<sup>3</sup>), the  $T_g$  (446–517 K), and

the  $E$  (5.70–8.63 GPa) values. We speculate that a combination of such heterogeneities in the nature of the interphase and the local  $T_g$  will play an important role in driving the formation of craze fibrils.<sup>28,42</sup> On the other hand, the use of pristine MWNTs to reinforce cross-linked epoxy will reduce the extent of these local thermomechanical heterogeneities, and reduce the likelihood of crazing compared to the use of A-MWNTs.<sup>28</sup>

**I. Thermal Conductivity Modestly Increases Due to Functionalization of the CNTs.** The thermal conductivity of the neat cross-linked epoxy and the three nanocomposite systems was calculated using the RNEMD method.<sup>41</sup> The time-averaged temperature profiles for the cross-linked epoxy and the epoxy–disp. FCNTs system, which were generated in response to the imposed heat flux in the RNEMD method,<sup>41</sup> are shown in Figure 8. As can be seen in that figure, the temperature difference between the hot and the cold regions in the cross-linked epoxy and the epoxy–disp. FCNTs system was 24 and 21 K, respectively. This temperature difference (not shown) in the case of the epoxy–disp. CNTs and the epoxy–agg. CNTs systems was 21 K. In addition, we note that the temperature profile that was established in response to the imposed heat flux in the case of all the four systems was approximately linear. This linearity allows us to assume that the thermal conductivity of a given model system was constant across the simulation box.

The calculated values of the thermal conductivity ( $k$ ) are shown in Table 4. Cross-linked epoxy has a thermal

**Table 4.** Thermal Conductivity Values for the Four Model Systems

system	thermal conductivity (W m <sup>-1</sup> K <sup>-1</sup> )
cross-linked epoxy	0.279 ± 0.009
epoxy–disp. CNTs	0.300 ± 0.01
epoxy–agg. CNTs	0.320 ± 0.01
epoxy–disp. FCNTs	0.363 ± 0.009

conductivity of 0.279 W m<sup>-1</sup> K<sup>-1</sup>, which is in reasonable agreement with the experimental value for the same system that was reported in literature<sup>69</sup> ( $k$  was approximately 0.2 W m<sup>-1</sup> K<sup>-1</sup>). The epoxy–disp. CNTs system exhibits ~8% enhancement in the thermal conductivity compared to the cross-linked epoxy. On the other hand, the epoxy–agg. CNTs system has a

higher thermal conductivity compared to the epoxy–disp. CNTs system, which suggests that the thermal resistance between the polymer matrix and the CNTs is higher than the thermal resistance between different CNTs. This trend in the values of  $k$  of the epoxy–disp. CNTs and the epoxy–agg. CNTs systems agrees with experimental results in literature,<sup>70</sup> where it was found that a reduction in the matrix–filler interfacial area results in an increase in the filler-induced enhancement of the thermal conductivity.

Furthermore, our results show that the epoxy–disp. FCNTs system has a somewhat higher value ( $\sim 21\%$ ) of the thermal conductivity compared to the epoxy–disp. CNTs system. In the case of the epoxy–disp. FCNTs system, there are two competing effects:

- (1) A reduction of the thermal resistance at the matrix–filler interface due to the presence of additional paths for phonon transfer.<sup>39,71</sup>
- (2) These additional paths can act as scattering points at the interface of CNTs, which will significantly reduce the intrinsic thermal conductivity of the CNTs, and hence tend to reduce that of the nanocomposite.<sup>70,72</sup>

Our result suggests that of the two competing effects mentioned above, the first effect dominates the thermal transport behavior of the epoxy–disp. FCNTs system. Similar observation of the enhancement in the value of  $k$  has been reported in literature<sup>73</sup> for cross-linked epoxy nanocomposites, where it was found using experiments that amine functionalized MWNTs in the nanocomposite resulted in a  $\sim 25\%$  improvement in the thermal conductivity compared to the nanocomposite containing pristine MWNTs. On the other hand, other work in literature reported that amine-functionalized CNTs were inferior to their pristine counterparts at enhancing the thermal conductivity of cross-linked epoxy in their nanocomposites.<sup>70</sup>

#### 4. CONCLUSIONS

In this work, the effect of using amido-amine functionalized CNTs on the properties of cross-linked epoxy nanocomposites was studied. The use of molecular simulations allowed us to compare properties of the epoxy nanocomposite containing pristine and functionalized CNTs, without changing the length of the CNTs, the extent of the conversion of the matrix, or the extent of dispersion of the filler. In particular, the extent of the dispersion of the FCNTs in the epoxy–disp. FCNTs system was the same as that of the pristine CNTs in the epoxy–disp. CNTs system, which was previously studied by us.<sup>11</sup> Thus, the differences in the thermo-mechanical properties of the two systems arise only because of the changes in the nature of the interphase region in the nanocomposite systems due to the functionalization of the CNTs.

The epoxy–disp. FCNTs system showed a value of the  $T_g$  that was comparable to that of the neat cross-linked epoxy. This trend was in contrast with the large  $T_g$  depression ( $\sim 66$  K) shown by the epoxy–disp. CNTs system compared to the neat cross-linked epoxy. Furthermore, the dependence of the excess specific volume between the epoxy–disp. CNTs and the epoxy–disp. FCNTs systems on the temperature indicated that the interphase between the matrix and the FCNTs in the epoxy–disp. FCNTs system is far less compressible than the interphase between the matrix and the pristine CNTs in the epoxy–disp. CNTs system. Thus, it can be concluded that the formation of covalent bonds between the matrix and the filler,

as is the case for the functionalized CNTs, is an effective strategy for reducing the compressibility of the matrix–filler interphase in nanocomposites.

An analysis of the dynamics of the matrix and the filler was performed by calculating the MSD values of the matrix atoms and the CNT atoms, respectively. The trends in the MSD of the matrix atoms show that the functionalization of the CNTs causes a large reduction in the mobility within the polymer matrix of the epoxy–disp. FCNTs system compared to that of the neat cross-linked epoxy and the epoxy–disp. CNTs systems. More importantly, the value of the MSD of the carbon atoms in the FCNTs shows a drastic reduction (more than an order of magnitude) compared to the corresponding value of the MSD in the epoxy–disp. CNTs system. This large reduction in the mobility of the CNT atoms suggests that the creation of covalent bonds between the matrix and the filler because of the functionalization of the CNTs has the effect of pinning the FCNTs in the matrix. Furthermore, this pinning of the FCNTs in the matrix couples the dynamics of the matrix and the filler, in contrast to the decoupling of the dynamics of the matrix and pristine CNTs in the epoxy–disp. CNTs system, as reported in our previous work.<sup>11</sup>

The mechanical properties of the four systems were characterized by simulating the uniaxial deformation of model structures of these, and thus calculating the Young's modulus and the Poisson ratio. It was observed that in spite of the presence of the stiff CNTs, the dispersed pristine CNTs caused no enhancement in the Young's modulus of the epoxy–disp. CNTs system compared to the neat cross-linked epoxy. This observation was attributed to the presence of the compressible interphase between the matrix and the CNTs in this system, which offsets the mechanical reinforcement due to the stiff CNTs. On the other hand, a reduction in the amount of this compressible interphase due to the aggregation of the CNTs resulted in  $\sim 12\%$  enhancement in the Young's modulus in the epoxy–agg. CNTs system compared to the neat cross-linked epoxy. Furthermore, the epoxy–disp. CNTs system showed a higher value of the Poisson ratio than that of the epoxy–agg. CNTs system. This trend in the value of the Poisson ratio indicates that the former is more ductile<sup>57</sup> than the latter. This pattern of behavior of the Young's modulus and the Poisson ratio is in agreement with experimental literature, which showed that the epoxy nanocomposite containing dispersed multiwalled CNTs was deemed to be more "liquid-like" compared to the nanocomposite containing aggregated multiwalled CNTs, which, in turn, was deemed to be more "solid-like".<sup>58</sup> In the case of the epoxy–disp. FCNTs system, the lower compressibility of the interphase between the matrix and the FCNTs compared to that of the epoxy–disp. CNTs system caused a large enhancement in the Young's modulus of the epoxy–disp. FCNTs system. The Young's modulus for this system was  $\sim 50\%$  higher than that of the neat cross-linked epoxy and the epoxy–disp. CNTs systems. The value of the Poisson ratio of this system was also lower than that of the other three systems.

Furthermore, these results also suggest a possible molecular mechanism for the observation of crazing and enhanced ductility in cross-linked epoxy nanocomposites containing amido-amine functionalized MWNTs that was reported in experimental literature.<sup>28</sup> In experimental systems of the nanocomposite containing functionalized CNTs, significant heterogeneities are expected in the local thermomechanical properties of the nanocomposite, which would manifest in large

variations in the value of the  $T_g$ , the compressibility of the matrix–filler interphase region, the Young's modulus, the Poisson ratio, and the extent of the dispersion of the filler. The neat cross-linked epoxy and the three nanocomposite systems studied by us represent these heterogeneous regions; our simulations show the differences in the  $T_g$  and the mechanical properties of the systems. These simulation results thus suggest that the heterogeneities in experimental samples of the functionalized CNTs used in nanocomposites can be expected to facilitate occurrence of crazing in cross-linked epoxy, which was recently reported in the literature.<sup>28</sup>

We also calculated the thermal conduction properties of the matrix, where the enhancement in the thermal conductivity was caused by the nature of the interphase region. In particular, while the thermal conductivity of the nanocomposite containing pristine well-dispersed CNTs only increased by ~8% compared to the neat cross-linked epoxy, the functionalization of the filler resulted in a ~21% enhancement in the thermal conductivity.

In this work, we were able to independently control the functionalization and the extent of dispersion of the CNTs because of the use of molecular simulations. This independent control enabled us to focus on the effect of the functionalization of the CNTs on the thermomechanical behavior of nanocomposites from the context of the nature of the interphase region surrounding the filler in the nanocomposite, which is difficult to study directly using experiments. In recent years, polymer–CNT interfacial strength has been investigated by analyzing contributions of various system components to the energy in simulations<sup>74</sup> or from a study of the forces involved in “pulling out” the filler from either the matrix or a filler agglomeration in experiments<sup>75</sup> and simulations.<sup>76–79</sup> We have used the ability of atomistic simulations to achieve a control over the degree of dispersion of the fillers in the polymer matrix without the use of additives such as stabilizer molecules. By comparing the volumetric, structural, dynamic, mechanical, and thermal transfer properties of nanocomposites of pristine and functionalized CNTs with the same loading and the degree of dispersion of the fillers, we have obtained insight into the role played by the CNT functionalization in governing the properties of the interphase region, which in turn, determine the overall properties of the nanocomposite.

The CNTs used in both the previous<sup>11</sup> and the present work are short compared to experiments and also have a small radius. Furthermore, we have not varied the aspect ratio of the CNTs, which can play an important role in designing practical applications. At this time, because of the limitations on the length-scales accessible by molecular simulations, factors such as the effect of the aspect ratio of the CNTs are best studied by experiments or multiscale modeling. However, we note that the matrix–filler interactions in polymer nanocomposites are not expected to be affected by the radius or the length of the CNTs.<sup>6</sup> Indeed, although the ability of CNTs to enhance matrix properties such as the fracture toughness<sup>28,42,80</sup> and damping characteristics<sup>76,81,82</sup> has proved promising, an atomistic scale understanding of the matrix–filler interactions will be crucial for further improvements. The ability of molecular simulations to explicitly account for the interatomic interactions and topology can provide insight into the molecular mechanisms that govern these phenomena in the nanocomposites. Such information of the molecular mechanisms derived from atomistic simulations, along with techniques of mesoscale modeling, and experiments, will

constitute a powerful tool kit for designing nanocomposite systems for material applications.<sup>83</sup>

## AUTHOR INFORMATION

### Corresponding Author

\*E-mail: rajesh.khare@ttu.edu. Phone: (806) 834-0449,

### Present Address

†Author K.S.K. is currently at the Howard P. Isermann Department of Chemical & Biological Engineering, and the Center for Biotechnology & Interdisciplinary Studies, Rensselaer Polytechnic Institute, Troy, New York 12180, United States.

### Notes

The authors declare no competing financial interest.

## ACKNOWLEDGMENTS

This material is based on work supported by the National Science Foundation under Grant: NSF CMMI 0900512. Any opinions, findings, and conclusions or recommendations expressed in this material are those of the authors and do not necessarily reflect the views of the National Science Foundation. The authors also acknowledge the Texas Advanced Computing Center (TACC) at The University of Texas at Austin for providing high-performance computing resources that have contributed to the research results reported within this paper.

## REFERENCES

- (1) Green, M. J.; Behabtu, N.; Pasquali, M.; Adams, W. W. Nanotubes as Polymers. *Polymer* **2009**, *50*, 4979–4997.
- (2) Špitalský, Z.; Tasis, D.; Papagelis, K.; Galiotis, C. Carbon Nanotube–Polymer Composites: Chemistry, Processing, Mechanical and Electrical Properties. *Prog. Polym. Sci.* **2010**, *35*, 357–401.
- (3) Tasis, D.; Tagmatarchis, N.; Bianco, A.; Prato, M. Chemistry of Carbon Nanotubes. *Chem. Rev.* **2006**, *106*, 1105–1136.
- (4) Bose, S.; Khare, R. A.; Moldenaers, P. Assessing the Strengths and Weaknesses of Various Types of Pre-treatments of Carbon Nanotubes on the Properties of Polymer/Carbon Nanotubes Composites: A Critical Review. *Polymer* **2010**, *51*, 975–993.
- (5) Schaefer, D. W.; Justice, R. S. How Nano Are Nanocomposites? *Macromolecules* **2007**, *40*, 8501–8517.
- (6) Grady, B. P. Effects of Carbon Nanotubes on Polymer Physics. *J. Polym. Sci., Part B: Polym. Phys.* **2012**, *50*, 591–623.
- (7) Moniruzzaman, M.; Winey, K. I. Polymer Nanocomposites Containing Carbon Nanotubes. *Macromolecules* **2006**, *39*, 5194–5205.
- (8) Li, X.; McKenna, G. B. Considering Viscoelastic Micromechanics for the Reinforcement of Graphene Polymer Nanocomposites. *ACS Macro Lett.* **2012**, *1*, 388–391.
- (9) Putz, K. W.; Palmeri, M. J.; Cohn, R. B.; Andrews, R.; Brinson, L. C. Effect of Cross-Link Density on Interphase Creation in Polymer Nanocomposites. *Macromolecules* **2008**, *41*, 6752–6756.
- (10) Allaoui, A.; El Bounia, N. How Carbon Nanotubes Affect the Cure Kinetics and Glass Transition Temperature of their Epoxy Composites? - A Review. *eXPRESS Polym. Lett.* **2009**, *3*, 588–594.
- (11) Khare, K. S.; Khare, R. Effect of Carbon Nanotube Dispersion on Glass Transition in Cross-Linked Epoxy–Carbon Nanotube Nanocomposites: Role of Interfacial Interactions. *J. Phys. Chem. B* **2013**, *117*, 7444–7454.
- (12) Kropka, J. M.; Pryamitsyn, V.; Ganesan, V. Relation between Glass Transition Temperatures in Polymer Nanocomposites and Polymer Thin Films. *Phys. Rev. Lett.* **2008**, *101*, 075702.
- (13) Jancar, J.; Douglas, J. F.; Starr, F. W.; Kumar, S. K.; Cassagnau, P.; Lesser, A. J.; Sternstein, S. S.; Buehler, M. J. Current Issues in Research on Structure–Property Relationships in Polymer Nanocomposites. *Polymer* **2010**, *51*, 3321–3343.

- (14) Starr, F. W.; Schröder, T. B.; Glotzer, S. C. Effects of a Nanoscopic Filler on the Structure and Dynamics of a Simulated Polymer Melt and the Relationship to Ultrathin Films. *Phys. Rev. E* **2001**, *64*, 021802.
- (15) Bansal, A.; Yang, H.; Li, C.; Cho, K.; Benicewicz, B. C.; Kumar, S. K.; Schadler, L. S. Quantitative Equivalence Between Polymer Nanocomposites and Thin Polymer Films. *Nat. Mater.* **2005**, *4*, 693–698.
- (16) Rittigstein, P.; Priestley, R. D.; Broadbelt, L. J.; Torkelson, J. M. Model Polymer Nanocomposites Provide an Understanding of Confinement Effects in Real Nanocomposites. *Nat. Mater.* **2007**, *6*, 278–282.
- (17) Ash, B. J.; Siegel, R. W.; Schadler, L. S. Glass Transition Temperature Behavior of Alumina/PMMA Nanocomposites. *J. Polym. Sci., Part B: Polym. Phys.* **2004**, *42*, 4371–4383.
- (18) Auad, M. L.; Mosiewicki, M. A.; Uzunpinar, C.; Williams, R. J. J. Functionalization of Carbon Nanotubes and Carbon Nanofibers used in Epoxy/Amine Matrices that Avoid Partitioning of the Monomers at the Fiber Interface. *Polym. Eng. Sci.* **2010**, *50*, 183–190.
- (19) Wang, S.; Liang, R.; Wang, B.; Zhang, C. Reinforcing Polymer Composites with Epoxide-Grafted Carbon Nanotubes. *Nanotechnology* **2008**, *19*, 085710.
- (20) González-Domínguez, J. M.; González, M.; Ansón-Casaos, A.; Díez-Pascual, A. M.; Gómez, M. A.; Martínez, M. T. Effect of Various Aminated Single-Walled Carbon Nanotubes on the Epoxy Cross-Linking Reactions. *J. Phys. Chem. C* **2011**, *115*, 7238–7248.
- (21) Wang, S.; Liang, Z.; Liu, T.; Wang, B.; Zhang, C. Effective Amino-Functionalization of Carbon Nanotubes for Reinforcing Epoxy Polymer Composites. *Nanotechnology* **2006**, *17*, 1551–1557.
- (22) Ma, P.-C.; Mo, S.-Y.; Tang, B.-Z.; Kim, J.-K. Dispersion, Interfacial Interaction and Re-agglomeration of Functionalized Carbon Nanotubes in Epoxy Composites. *Carbon* **2010**, *48*, 1824–1834.
- (23) Ma, P.-C.; Siddiqui, N. A.; Marom, G.; Kim, J.-K. Dispersion and Functionalization of Carbon Nanotubes for Polymer-based Nanocomposites: A Review. *Composites, Part A* **2010**, *41*, 1345–1367.
- (24) Ma, P.-C.; Zheng, Q.-B.; Mäder, E.; Kim, J.-K. Behavior of Load Transfer in Functionalized Carbon Nanotube/Epoxy Nanocomposites. *Polymer* **2012**, *53*, 6081–6088.
- (25) Sun, L.; Warren, G. L.; O'Reilly, J. Y.; Everett, W. N.; Lee, S. M.; Davis, D.; Lagoudas, D.; Sue, H. J. Mechanical Properties of Surface-Functionalized SWCNT/Epoxy Composites. *Carbon* **2008**, *46*, 320–328.
- (26) Martínez-Rubi, Y.; González-Domínguez, J. M.; Ansón-Casaos, A.; Kingston, C. T.; Daroszewska, M.; Barnes, M.; Hubert, P.; Cattin, C.; Martínez, M. T.; Simard, B. Tailored SWCNT Functionalization Optimized for Compatibility with Epoxy Matrices. *Nanotechnology* **2012**, *23*, 285701.
- (27) Gojny, F. H.; Nastalczyk, J.; Roslaniec, Z.; Schulte, K. Surface Modified Multi-walled Carbon Nanotubes in CNT/Epoxy-Composites. *Chem. Phys. Lett.* **2003**, *370*, 820–824.
- (28) Zhang, W.; Srivastava, I.; Zhu, Y.-F.; Picu, C. R.; Koratkar, N. A. Heterogeneity in Epoxy Nanocomposites Initiates Crazing: Significant Improvements in Fatigue Resistance and Toughening. *Small* **2009**, *5*, 1403–1407.
- (29) Saito, T.; Matsushige, K.; Tanaka, K. Chemical Treatment and Modification of Multi-walled Carbon Nanotubes. *Phys. B* **2002**, *323*, 280–283.
- (30) Špitalský, Z.; Matějka, L.; Šlouf, M.; Konyushenko, E. N.; Kovářová, J.; Zemek, J.; Kotek, J. Modification of Carbon Nanotubes and its Effect on Properties of Carbon Nanotube/Epoxy Nanocomposites. *Polym. Compos.* **2009**, *30*, 1378–1387.
- (31) Grillet, A. C.; Galy, J.; Gérard, J.-F.; Pascault, J.-P. Mechanical and Viscoelastic Properties of Epoxy Networks Cured with Aromatic Diamines. *Polymer* **1991**, *32*, 1885–1891.
- (32) Alcoutlabi, M.; McKenna, G. B. Effects of Confinement on Material Behaviour at the Nanometre Size Scale. *J. Phys.: Condens. Matter* **2005**, *17*, 461–524.
- (33) Grady, B. P. Thermal Conductivity. In *Carbon Nanotube–Polymer Composites: Manufacture, Properties, and Applications*; John Wiley & Sons: New York, 2011; pp 283–304.
- (34) Hone, J.; Whitney, M.; Piskoti, C.; Zettl, A. Thermal Conductivity of Single-Walled Carbon Nanotubes. *Phys. Rev. B* **1999**, *59*, R2514–R2516.
- (35) Kim, P.; Shi, L.; Majumdar, A.; McEuen, P. L. Thermal Transport Measurements of Individual Multiwalled Nanotubes. *Phys. Rev. Lett.* **2001**, *87*, 215502.
- (36) Duong, H. M.; Yamamoto, N.; Bui, K.; Papavassiliou, D. V.; Maruyama, S.; Wardle, B. L. Morphology Effects on Nonisotropic Thermal Conduction of Aligned Single-Walled and Multi-Walled Carbon Nanotubes in Polymer Nanocomposites. *J. Phys. Chem. C* **2010**, *114*, 8851–8860.
- (37) Peterson, R. E.; Anderson, A. C. The Kapitza Thermal Boundary Resistance. *J. Low Temp. Phys.* **1973**, *11*, 639–665.
- (38) Duong, H. M.; Papavassiliou, D. V.; Mullen, K. J.; Maruyama, S. Computational Modeling of the Thermal Conductivity of Single-walled Carbon Nanotube–Polymer Composites. *Nanotechnology* **2008**, *19*, 065702.
- (39) Varshney, V.; Roy, A. K.; Michalak, T. J.; Lee, J.; Farmer, B. L. Effect of Curing and Functionalization on the Interface Thermal Conductance in Carbon Nanotube-Epoxy Composites. *JOM* **2013**, *65*, 140–146.
- (40) Khare, K. S.; Khare, R. Directed Diffusion Approach for Preparing Atomistic Models of Crosslinked Epoxy for Use in Molecular Simulations. *Macromol. Theory Simul.* **2012**, *21*, 322–327.
- (41) Müller-Plathe, F. A Simple Nonequilibrium Molecular Dynamics Method for Calculating the Thermal Conductivity. *J. Chem. Phys.* **1997**, *106*, 6082–6085.
- (42) Srivastava, I.; Koratkar, N. Fatigue and Fracture Toughness of Epoxy Nanocomposites. *JOM* **2010**, *62*, 50–57.
- (43) Wang, J.; Wang, W.; Kollman, P. A.; Case, D. A. Automatic Atom Type and Bond Type Perception in Molecular Mechanical Calculations. *J. Mol. Graphics Modell.* **2006**, *25*, 247–260.
- (44) Wang, J.; Wolf, R. M.; Caldwell, J. W.; Kollman, P. A.; Case, D. A. Development and Testing of a General AMBER Force Field. *J. Comput. Chem.* **2004**, *25*, 1157–1174.
- (45) Jakalian, A.; Bush, B. L.; Jack, D. B.; Bayly, C. I. Fast, Efficient Generation of High-Quality Atomic Charges. AM1-BCC Model: I. Method. *J. Comput. Chem.* **2000**, *21*, 132–146.
- (46) Jakalian, A.; Jack, D. B.; Bayly, C. I. Fast, Efficient Generation of High-Quality Atomic Charges. AM1-BCC Model: II. Parameterization and Validation. *J. Comput. Chem.* **2002**, *23*, 1623–1641.
- (47) Lin, P.-H.; Khare, R. Local Chain Dynamics and Dynamic Heterogeneity in Cross-Linked Epoxy in the Vicinity of Glass Transition. *Macromolecules* **2010**, *43*, 6505–6510.
- (48) Lin, P.-H.; Khare, R. Molecular Simulation of Cross-Linked Epoxy and Epoxy-POSS Nanocomposite. *Macromolecules* **2009**, *42*, 4319–4327.
- (49) Soni, N. J.; Lin, P.-H.; Khare, R. Effect of Cross-linker Length on the Thermal and Volumetric Properties of Cross-linked Epoxy Networks: A Molecular Simulation Study. *Polymer* **2012**, *53*, 1015–1019.
- (50) Sirk, T. W.; Khare, K. S.; Karim, M.; Lenhart, J. L.; Andzelm, J. W.; McKenna, G. B.; Khare, R. High Strain Rate Mechanical Properties of a Cross-linked Epoxy Across the Glass Transition. *Polymer* **2013**, *54*, 7048–7057.
- (51) Hockney, R. W.; Eastwood, J. W. *Computer Simulation Using Particles*; Institute of Physics Publishing: Philadelphia, 1988; pp 267–301.
- (52) Shinoda, W.; Shiga, M.; Mikami, M. Rapid Estimation of Elastic Constants by Molecular Dynamics Simulation Under Constant Stress. *Phys. Rev. B* **2004**, *69*, 134103.
- (53) Plimpton, S. Fast Parallel Algorithms for Short-Range Molecular Dynamics. *J. Comput. Phys.* **1995**, *117*, 1–19.
- (54) Tuckerman, M. E.; Alejandre, J.; López-Rendón, R.; Jochim, A. L.; Martyna, G. J.; Liouville-Operator, A. Derived Measure-Preserving

Integrator for Molecular Dynamics Simulations in the Isothermal–Isobaric Ensemble. *J. Phys. A: Math. Gen.* **2006**, *39*, 5629.

(55) Godawat, R.; Jamadagni, S. N.; Garde, S. Characterizing Hydrophobicity of Interfaces by using Cavity Formation, Solute Binding, and Water Correlations. *Proc. Natl. Acad. Sci. U.S.A.* **2009**, *106*, 15119–15124.

(56) Halary, J.-L.; Lauprêtre, F.; Monnerie, L. *Polymer Materials: Macroscopic Properties and Molecular Interpretations*; Wiley: Hoboken, NJ, 2011.

(57) Greaves, G. N.; Greer, A. L.; Lakes, R. S.; Rouxel, T. Poisson's Ratio and Modern Materials. *Nat. Mater.* **2011**, *10*, 823–37.

(58) Song, Y. S.; Youn, J. R. Influence of Dispersion States of Carbon Nanotubes on Physical Properties of Epoxy Nanocomposites. *Carbon* **2005**, *43*, 1378–1385.

(59) Green, M. J. Analysis and Measurement of Carbon Nanotube Dispersions: Nanodispersion versus Macrodispersion. *Polym. Int.* **2010**, *59*, 1319–1322.

(60) Riggleman, R. A.; Toepperwein, G. N.; Papakonstantopoulos, G. J.; de Pablo, J. J. Dynamics of a Glassy Polymer Nanocomposite during Active Deformation. *Macromolecules* **2009**, *42*, 3632–3640.

(61) Affdl, J. C. H.; Kardos, J. L. The Halpin-Tsai Equations: A Review. *Polym. Eng. Sci.* **1976**, *16*, 344–352.

(62) Ferry, J. *Viscoelastic Properties of Polymers*, 3rd ed.; Wiley: New York, 1980; p xxiv.

(63) O'Connell, P. A.; McKenna, G. B. Yield and Crazing in Polymers. In *Encyclopedia of Polymer Science and Technology*; John Wiley & Sons: New York, 2002.

(64) Gent, A. N. Hypothetical Mechanism of Crazing in Glassy Plastics. *J. Mater. Sci.* **1970**, *5*, 925–932.

(65) Toepperwein, G. N.; de Pablo, J. J. Cavitation and Crazing in Rod-Containing Nanocomposites. *Macromolecules* **2011**, *44*, 5498–5509.

(66) Kinloch, A. J.; Williams, J. G. Crack Blunting Mechanisms in Polymers. *J. Mater. Sci.* **1980**, *15*, 987–996.

(67) Becu, L.; Maazouz, A.; Sautereau, H.; Gerard, J. F. Fracture Behavior of Epoxy Polymers Modified with Core-Shell Rubber Particles. *J. Appl. Polym. Sci.* **1997**, *65*, 2419–2431.

(68) Azimi, H. R.; Pearson, R. A.; Hertzberg, R. W. Fatigue of Hybrid Epoxy Composites: Epoxies Containing Rubber and Hollow Glass Spheres. *Polym. Eng. Sci.* **1996**, *36*, 2352–2365.

(69) Giang, T.; Park, J.; Cho, I.; Ko, Y.; Kim, J. Effect of Backbone Moiety in Epoxies on Thermal Conductivity of Epoxy/Alumina Composite. *Polym. Compos.* **2013**, *34*, 468–476.

(70) Gojny, F. H.; Wichmann, M. H. G.; Fiedler, B.; Kinloch, I. A.; Bauhofer, W.; Windle, A. H.; Schulte, K. Evaluation and Identification of Electrical and Thermal Conduction Mechanisms in Carbon Nanotube/Epoxy Composites. *Polymer* **2006**, *47*, 2036–2045.

(71) Roy, A. K.; Farmer, B. L.; Varshney, V.; Sih, S.; Lee, J.; Ganguli, S. Importance of Interfaces in Governing Thermal Transport in Composite Materials: Modeling and Experimental Perspectives. *ACS Appl. Mater. Interfaces* **2012**, *4*, 545–563.

(72) Shenogin, S.; Bodapati, A.; Xue, L.; Ozisik, R.; Keblinski, P. Effect of Chemical Functionalization on Thermal Transport of Carbon Nanotube Composites. *Appl. Phys. Lett.* **2004**, *85*, 2229–2231.

(73) Yang, K.; Gu, M. The Effects of Triethylenetetramine Grafting of Multi-Walled Carbon Nanotubes on its Dispersion, Filler-Matrix Interfacial Interaction and the Thermal Properties of Epoxy Nanocomposites. *Polym. Eng. Sci.* **2009**, *49*, 2158–2167.

(74) Huang, J. C.; Chiu, C. Y. The Study of Single-walled Nanotube Reinforced Epoxy Composites by Molecular Dynamics. *Polym. Polym. Composites* **2011**, *19*, 377–382.

(75) Manoharan, M. P.; Sharma, A.; Desai, A. V.; Haque, M. A.; Bakis, C. E.; Wang, K. W. The Interfacial Strength of Carbon Nanofiber Epoxy Composite using Single Fiber Pullout Experiments. *Nanotechnology* **2009**, *20*, 295701.

(76) Liu, A.; Wang, K. W.; Bakis, C. E. Effect of Functionalization of Single-wall Carbon Nanotubes (SWNTs) on the Damping Characteristics of SWNT-based Epoxy Composites via Multiscale Analysis. *Composites, Part A* **2011**, *42*, 1748–1755.

(77) Liu, A.; Wang, K. W.; Bakis, C. E. Multiscale Damping Model for Polymeric Composites Containing Carbon Nanotube Ropes. *J. Compos. Mater.* **2010**, *44*, 2301–2323.

(78) Liao, K.; Li, S. Interfacial Characteristics of a Carbon Nanotube–Polystyrene Composite System. *Appl. Phys. Lett.* **2001**, *79*, 4225–4227.

(79) Gou, J.; Liang, Z.; Zhang, C.; Wang, B. Computational Analysis of Effect of Single-walled Carbon Nanotube Rope on Molecular Interaction and Load Transfer of Nanocomposites. *Composites, Part B* **2005**, *36*, 524–533.

(80) Zhu, Y.; Bakis, C. E.; Adair, J. H. Effects of Carbon Nanofiller Functionalization and Distribution on Interlaminar Fracture Toughness of Multi-scale Reinforced Polymer Composites. *Carbon* **2012**, *50*, 1316–1331.

(81) Zhou, X.; Shin, E.; Wang, K. W.; Bakis, C. E. Interfacial Damping Characteristics of Carbon Nanotube-based Composites. *Compos. Sci. Technol.* **2004**, *64*, 2425–2437.

(82) Jonghwan, S.; Koratkar, N.; Keblinski, P.; Ajayan, P. Viscoelasticity in Carbon Nanotube Composites. *Nat. Mater.* **2005**, *4*, 134–137.

(83) Schadler, L. S.; Kumar, S. K.; Benicewicz, B. C.; Lewis, S. L.; Harton, S. E. Designed Interfaces in Polymer Nanocomposites: A Fundamental Viewpoint. *MRS Bull.* **2007**, *32*, 335–340.